trans isomer, and increased donation from the nonplanar *N*-amido ligands in the cis-α ligand complements, which stabilizes the cis-α isomer in the more oxidized complexes. The increased donation probably also destabilizes the cis-α isomer in the more reduced species. The increase in ligand–metal bonding in the stable cis-α complexes is probably substantial, since rotational processes around the C–N bond of organic amides are typically subject to large activation barriers (10–35 kcal·mol^{-1}).[31] Note that these results imply that the trans to cis-α isomerizations occur so that nonplanar amido ligands can be produced rather than in spite of the production of nonplanar *N*-amido ligands.

An unexpected ligand design principle is implicit in this work. If *N*-amido PAC ligands are being designed to produce highly oxidizing metal complexes, then it might be important to design the PAC ligands such that spontaneous formation of nonplanar *N*-amido ligands cannot occur. Incorporation of the *N*-amido ligand in a relatively inflexible macrocyclic ligand might be a sufficient constraint.

(31) Stewart, W. E.; Siddall, T. H., III *Chem. Rev.* **1970**, *70*, 517–551.

A New Magic Cluster Electron Count and Metal–Metal Multiple Bonding

Ralph A. Wheeler and Roald Hoffmann*

Contribution from the Department of Chemistry and Materials Science Center, Cornell University, Ithaca, New York 14853-1301. Received May 5, 1986

Abstract: Metal–metal multiple bonding radically alters the preferred electron count for trigonal-prismatic clusters. The recently synthesized Tc$_6$Cl$_{12}^{2-}$ and Tc$_6$Cl$_{14}^{3-}$ have short Tc–Tc bonds parallel to the prism's threefold axis. Tc$_6$Cl$_{12}^{2-}$ has 32 metal electrons and Tc$_6$Cl$_{14}^{3-}$ has 31. A molecular orbital analysis of the bonding in Tc$_6$Cl$_{12}^{2-}$ shows essentially electron rich ($\sigma^2\pi^4\delta^2\delta^{*2}$) triple bonding within each dimer unit, single bonds in the triangles, and two electrons in an a$_2''$ orbital that is π^* with respect to the dimers, weakly bonding in the triangles. The a$_2''$ is net antibonding, so that the number of framework bonding electrons in this structure is only 30. This is a very different magic number from the 16, 24, or 14 known for octahedra and 18 for trigonal prisms. One-electron oxidation affects Tc$_6$Cl$_{14}^{3-}$ bonding in a predictable way; we also discuss the Tc$_8$Br$_{12}$ structure.

Kryuchkov, Kuzina, and Spitsyn recently synthesized two Tc clusters, Tc$_6$Cl$_{12}^{2-}$ and Tc$_6$Cl$_{14}^{3-}$ (**1** and **2**),[1a-d] which stand at the intersection of two important directions of modern inorganic chemistry—namely, cluster chemistry and metal–metal multiple bonding.

(1) (a) Kryuchkov, S. V.; Kuzina, A. F.; Spitsyn, V. I. *Dokl. Akad. Nauk SSSR* **1982**, *266*, 127; *Dokl. Akad. Nauk SSSR* (*Engl. Transl.*) **1982**, *266*, 304. (b) German, K. E.; Kryuchkov, S. V.; Kuzina, A. F.; Spitsyn, V. I. *Dokl. Akad. Nauk SSSR* **1986**, *288*, 381. (c) Spitsyn, V. I.; Kuzina, A. F.; Oblova, A. A.; Kryuchkov, S. V. *Uspek. Khim.* **1985**, *54*, 637; *Russ. Chem. Rev.* **1985**, *54*, 373. (d) For a related octahedral cluster see: Kryuchkov, S. V.; Kuzina, A. F.; Spitsyn, V. I. *Dokl. Akad. Nauk SSSR* **1986**, *287*, 1400. (e) Koz'min, P. A.; Surazhskaya, M. D.; Larina, T. B. *Koord. Khim.* **1985**, *11*, 1559. (f) Koz'min, P. A.; Surazhskaya, M. D.; Larina, T. B. *Dokl. Akad. Nauk SSSR* **1983**, *271*, 1157.

Tc$_6$Cl$_{12}^{2-}$ Tc$_6$Cl$_{14}^{3-}$

1   **2**
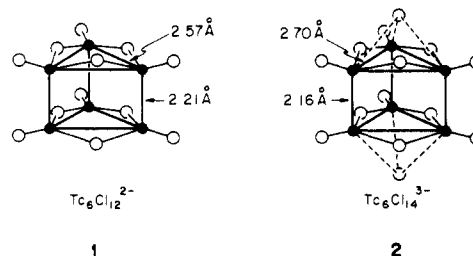
Let us first describe these compounds, whose structures were determined by Koz'min, Surazhskaya, and Larina,[1e,f] and then pinpoint their significance. **1** and **2** are both trigonal prisms of metal atoms. In each, every technetium has one terminal chloride;

six chlorides also bridge the edges bordering triangular prism faces. In **2** there are two additional chlorides roughly along the threefold axis and a long 3 Å from the Tc. If these were thought of as nonbonded, **2** would be $Tc_6Cl_{12}^-$, with one electron less than **1**.

The Tc–Tc distances in **1** and **2** are remarkably short. In **1** they are 2.57 Å on the triangular faces, 2.21 Å parallel to the prism axis. By removing one electron on going to **2**, the short Tc–Tc distance contracts still more, to 2.16 Å and the triangular face distance stretches to 2.70 Å.

The very short prism distances indicate metal–metal multiple bonding, as they do in another remarkable cluster synthesized by the same group, Tc_8Br_{12}, **3**.[1a,c,2]
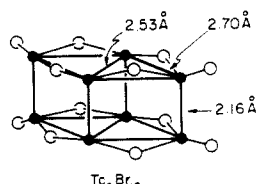
3

The exceptional synthetic, structural, mechanistic, and theoretical construct of metal–metal multiple bonding is a high point of modern inorganic chemistry that we owe to Cotton.[3] The origins of the concept lie in the chemistry of $Re_2Cl_8^{2-}$, and most of the work in this incredibly interesting area has been on binuclear complexes. But there have been some indications of multiple bonding in higher nuclearity aggregates, e.g., $Re_3Cl_9L_3$ and the clusters discussed next, which move toward the technetium prisms.

In 1978, McCarley provided a harbinger of new cluster chemistry when he reported the synthesis and X-ray structure of $Mo_4Cl_8(PEt_3)_4$, **4**.[4,6i] The molecule is a rectangle of Mo atoms in square pyramidal coordination environments. The short Mo–
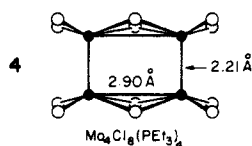
Mo distance, 2.21 Å, represents a typical Mo–Mo triple bond length.[5] Giving each Cl a 1– formal charge prompted McCarley to assign the sixteen d electrons to localized metal–metal bonds—single bonds along the rectangle's long sides and triple bonds on the shorter edges. The Mo≡Mo triple bonds in $Mo_4Cl_8(PEt_3)_4$ are remarkable because they suggest the possibility of other clusters containing metal–metal multiple bonds.

Since McCarley's discovery, a number of tetranuclear clusters, some with M–M multiple bonds and some without, were isolated in a variety of geometries.[6]

Table I. Examples of Six-Vertex Transition-Metal Clusters, Their Electron Counts, and Their Geometries

| molecule | number of electrons | | | geometry |
	cluster	metal	metal–metal bonding	
$Zr_6I_{14}C$	84	14	14	octahedron
$Ta_6Cl_{12}^{2+}$- $(Ta_6Cl_{18}^{4-})$	64 (76)	16	16	octahedron
$Mo_6Cl_8^{4+}$- $(Mo_6Cl_{14}^{2-})$	72 (84)	24	24	octahedron
$Tc_6Cl_{12}^{2-}$	68	32	30	trigonal prism
$Os_6(CO)_{18}^{2-}$	86	50	14	octahedron
$Rh_6(CO)_{16}$	86	54	14	octahedron
$Rh_6C(CO)_{15}^{2-}$	90	60	18	trigonal prism
$Ni_6(CO)_{12}^{2-}$	86	62	14	trigonal antiprism
$Pt_6(CO)_{12}^{2-}$	86	62	14	trigonal prism

That brings us to the technetium clusters from the metal–metal multiple bonding side. Clearly they have short bonds, and just as clearly they are clusters, in the shape of trigonal prisms. Now another major stream in contemporary inorganic chemistry is that of clusters. We have had a fantastic variety of polyhedral shapes put before us, among them many six vertex octahedral and trigonal prismatic species. And the exciting experimental developments have been accompanied by the most important theoretical inorganic development of the seventies, the skeletal electron pair counting rules of Mingos and of Wade.[7] These allow the association of a total cluster electron count, or a specific number of bonding pairs, with a given cluster geometry. Table I lists some representative six-vertex clusters and their characteristic electron counts.

Consider for instance the octahedral $Os_6(CO)_{18}^{2-}$, **5**,[8] and the trigonal prismatic $Rh_6C(CO)_{15}^{2-}$ **6**.[9] The total electron count (including two electrons contributed to cluster bonding by each

$Os_6(CO)_{18}^{2-}$ $Rh_6(CO)_{15}C^{2-}$
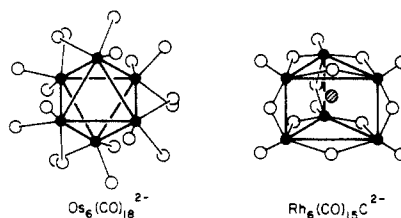
5   **6**

carbonyl, no matter whether terminal or bridging) in **5** is 86, and in **6** it is 90. Most of these electrons are involved in metal-ligand bonding or are nonbonding at the metal. The frameworks are held together by a characteristic 14 electrons for the octahedron, 18 for the trigonal prism.

Note should be taken here of a certain ambiguity in electron counting, of which workers in the field are aware. The total number of cluster electrons is (relatively) unambiguous, and so is the number of framework bonding electrons. But metal electrons can be traded for ligand electrons apparently quite freely. Witness the existence of $Os_6(CO)_{18}^{2-}$ and $Rh_6(CO)_{16}$,[10] both having 86 electrons, 14 metal–metal bonding electrons, but obviously different metal and ligand electron counts.

(2) (a) Koz'min, P. A.; Surazhskaya, M. D.; Larina, T. B. *Dokl. Akad. Nauk SSSR* **1982**, *265*, 1420; *Dokl. Akad. Nauk SSSR (Engl. Transl.)* **1983**, *265*, 656. (b) Kryuchkov, S. V.; Grigoryev, M. S.; Kuzina, A. F.; Gulyev, B. F.; Spitsyn, V. I. *Dokl. Akad. Nauk SSSR*, **1986**, *288*, 893.

(3) (a) Cotton, F. A.; Walton, R. A. *Multiple Bonds Between Metal Atoms*; Wiley-Interscience: New York, 1982. (b) Cotton, F. A.; Walton, R. A. *Struc. Bonding* **1985**, *62*, 1.

(4) McGinnis, R. N.; Ryan, T. R.; McCarley, R. E. *J. Am. Chem. Soc.* **1978**, *100*, 7900.

(5) Cotton, F. A. *J. Less-Common Met.* **1977**, *54*, 3.

(6) (a) Cotton, F. A.; Powell, G. L. *Inorg. Chem.* **1983**, *22*, 871. (b) Chisholm, M. H.; Errington, R. J.; Folting, K.; Huffman, J. C. *J. Am. Chem. Soc.* **1982**, *104*, 2025. (c) Chisholm, M. H.; Huffman, J. C.; Kelly, R. L. *J. Am. Chem. Soc.* **1979**, *101*, 7100. (d) Chisholm, M. H.; Huffman, J. C.; Kirkpatrick, C. C.; Leonelli, J.; Folting, K. *J. Am. Chem. Soc.* **1981**, *103*, 6093. (e) Chisholm, M. H.; Huffman, J. C.; Leonelli, J. *J. Am. Chem. Soc., Chem. Commun.* **1981**, 270. (f) Akiyama, M.; Chisholm, M. H.; Cotton, F. A.; Extine, M. W.; Haitko, D. A.; Leonelli, J.; Little, D. *J. Am. Chem. Soc.* **1981**, *103*, 779. (g) Torardi, C. C.; McCarley, R. E. *J. Solid State Chem.* **1981**, *37*, 393. (h) McCarley, R. E.; Luly, M. H.; Ryan, T. R.; Torardi, C. C. *ACS Symp. Ser.* **1981**, *155*, 41. (i) Aufdembrink and McCarley recently reported the structures of the two isomers of $Mo_4Cl_{12}^{3-}$. One is a planar rectangle with two chlorides bridging each edge and Mo–Mo distances of 2.358 and 2.653 Å. The other is a butterfly cluster: Aufdembrink, B. A.; McCarley, R. E. *J. Am. Chem. Soc.* **1986**, *108*, 2474.

(7) (a) Mingos, D. M. P. *Acc. Chem. Res.* **1984**, *17*, 311. (b) Mingos, D. M. P. In *Comprehensive Organometallic Chemistry*; Wilkinson, G., Stone, F. G. A., Abel, E. W., Eds.; Pergamon: Oxford, 1981. (c) Mason, R.; Mingos, D. M. P. *MTP Int. Rev. Sci.: Phys. Chem., Ser. Two* **1975**, *11*, 121. (d) Wade, K. *Adv. Inorg. Chem. Radiochem.* **1976**, *18*, 1. (e) Wade, K. *Chem. Br.* **1975**, *11*, 177. (f) Wade, K. *J. Chem. Soc., Chem. Commun.* **1971**, 792. (g) Wade, K. *Inorg. Nucl. Chem. Lett.* **1972**, *8*, 559, 563. (h) Wade, K. *Electron Deficient Compounds*; Nelson: London, 1971. (i) Mingos, D. M. P. *Nature (London)*, *Phys. Sci.* **1972**, *236*, 99.

(8) McPartlin, M.; Eady, C. R.; Johnson, B. F. G.; Lewis, J. *J. Chem. Soc., Chem. Commun.* **1976**, 883.

(9) Albano, V. G.; Sansoni, M.; Chini, P.; Martinengo, S. *J. Chem. Soc., Dalton Trans.* **1973**, 651.

(10) Corey, E. R.; Dahl, L. F.; Beck, W. *J. Am. Chem. Soc.* **1963**, *85*, 1202.

These are not the only electron counts characteristic of these geometries. For instance ubiquitous octahedral face-capped M_6X_8, 7, and edge-bridged M_6X_{12} clusters, 8, are important in early transition-metal chemistry.[11] These often have six additional terminal ligands. One has to be careful with electron counting in these clusters. The terminal ligands are two-electron donors, but face-capping S^{2-} or Cl^- are best thought of as donating six

$\{[M_6X_8]X_6\}^{2-}$ 　　　　　$\{[M_6X_{12}]X_6\}^{4-}$

M = Mo, W 　　　　　　　　　M = Nb, Ta

7 　　　　　　　　　　　　　　　8
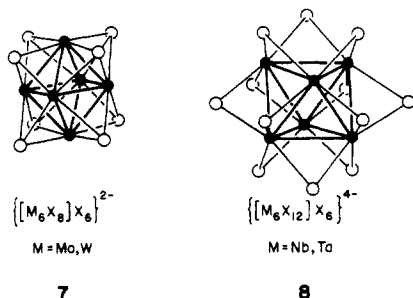
electrons to the cluster, and edge-bridging Cl^- as donating four. With these conventions one reaches electron counts of 72 for M_6X_8 (or 84 for $M_6X_6L_6$) and 64 for M_6X_{12} (or 76 for $M_6X_{12}L_6$). Whatever the number of terminal ligands, the magic electron counts for the polyhedra are clear—they are 24 metal–metal bonding electrons for M_6X_8[12] and 16 for M_6X_{12}.[12b,13] These are well understood and have been discussed in conjunction with preferred electron counts for the octahedral transition-metal carbonyl clusters.[14] The alternative possibility of a 14-electron count in some centered $M_6X_{12}Y$ clusters is also clear.[15]

Even if we limit ourselves to six-vertex clusters this does not exhaust the available molecules. $Ni_6(CO)_{12}^{2-}$ with 86 electrons is trigonal antiprismatic, near to octahedral.[16a] But $Pt_6(CO)_{12}^{2-}$, with the same electron count, is close to a trigonal prism.[16b] The bonding in these late transition-metal clusters is described elsewhere.[16c] And six-vertex clusters are not only octahedral and trigonal prismatic. Other topologies occur.[17]

In the context of octahedral or trigonal prismatic clusters—the best studied group of clusters that we have—$Tc_6Cl_{12}^{2-,1-}$ presents an unusual, novel electron count, quite apart from its structural interest. If we count the bridging chlorides as contributing four electrons to the cluster and the terminal ones as giving two, we come to an electron count of 68. This is a new number. And how many of these electrons are involved in metal–metal bonding? That is the subject of this contribution.

M≡M Dimers: $Mo_4Cl_8(PEt_3)_4$

We begin our analysis with $Mo_4Cl_8(PEt_3)_4$, not because the molecule holds any surprises but because orbital features that are

(11) (a) Simon, A. *Angew. Chem.* **1981**, *93*, 23; *Angew. Chem., Intl. Ed. Engl.* **1981**, *20*, 1. (b) McCarley, R. E. *Phil. Trans R. Soc. (London)* **1982**, *308*, 141. (c) Corbett, J. D. *J. Solid State Chem.* **1981**, *37*, 335.

(12) For leading references, see: (a) Nohl, H.; Klose, W.; Andersen, O. K.; Kelly, P. J. In *Superconductivity in Ternary Compounds I*; Fischer, Ø., Maple, M. B., Eds.; Springer-Verlag: New York, 1982; Chapter 6. (b) Bursten, B. E.; Cotton, F. A.; Stanely, G. G. *Isr. J. Chem.* **1980**, *19*, 132.

(13) (a) Korol'kov, D. V.; Pak, V. N. *Zh. Strukt. Khim.* **1971**, *12*, 310; *J. Struct. Chem.* **1971**, *12*, 282. (b) Voronovich, N. S.; Korol'kov, D. V. *Kh. Strukt. Khim.* **1971**, *12*, 501, 676; *J. Struct. Chem.* **1971**, *12*, 458, 613. (c) Kettle, S. F. A. *Theor. Chim. Acta* **1965**, *3*, 210. (d) Cotton, F. A.; Haas, T. E. *Inorg. Chem.* **1964**, *3*, 210. (e) Crossman, C. D.; Olsen, D. P.; Duffey, G. H. *J. Chem. Phys.* **1963**, *38*, 73. (f) Duffey, G. H. *J. Chem. Phys.* **1951**, *19*, 963.

(14) Johnston, R. L.; Mingos, D. M. P. *Inorg. Chem.* **1986**, *25*, 1661.

(15) (a) Smith, J. D.; Corbett, J. D. *J. Am. Chem. Soc.* **1985**, *107*, 5704. (b) Ziebarth, R. P.; Corbett, J. D. *J. Am. Chem. Soc.* **1985**, *107*, 4571.

(16) (a) Calabrese, J. C.; Dahl, L. F.; Cavalieri, A.; Chini, P.; Longoni, G.; Martinengo, S. *J. Am. Chem. Soc.* **1974**, *96*, 2616. (b) Calabrese, J. C.; Dahl, L. F.; Cavalieri, A.; Chini, P.; Longoni, G.; Martinengo, S. *Ibid.* **1974**, *96*, 2614. (c) Underwood, D. J.; Hoffmann, R.; Tatsumi, K.; Nakamura, A.; Yamamoto, Y. *J. Am. Chem. Soc.* **1985**, *107*, 5968 and references therein.

(17) (a) Raithby, P. R. In *Transition Metal Clusters*; Johnson, B. F. G., Ed.; Wiley-Interscience: New York, 1980. (b) Johnson, B. F. G.; Lewis, J. *Adv. Inorg. Chem. Radiochem.* **1981**, *24*, 225. (c) Benfield, R. E.; Johnson, B. F. G. *Top. Stereochem.* **1981**, *12*, 253. (d) Chini, P.; Longoni, G.; Albano, V. G. *Adv. Organomet. Chem.* **1976**, *14*, 285. (e) Lewis, J.; Johnson, B. F. G. *Pure Appl. Chem.* **1982**, *54*, 97. (f) Mingos, D. M. P. *Chem. Soc. Rev.* **1986**, *15*, 31.
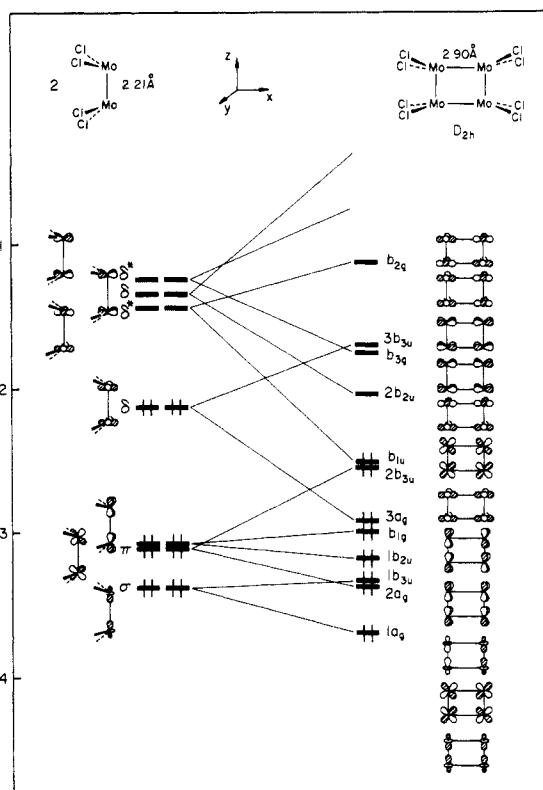
Figure 1. Interaction of two $Cl_2Mo\equiv MoCl_2$ units to form Mo_4Cl_8.

Table II. Orbital Occupations of Mo_2 Fragment Orbitals

molecule (fragment)	orbital occupations					
	σ	π	δ	δ^*	π^*	σ^*
(Mo_2Cl_4)	1.99	3.99	2.35	0.45	0.25	0.18
(Mo_4Cl_8)	1.99	3.94	1.36	0.94	0.45	0.38
$Mo_4Cl_{12}^{4-}$	1.99	3.95	1.75	1.59	0.49	0.30
$Mo_2Cl_8^{6-}$ ^{a}	1.98	4.00	2.52	2.49	0.48	0.27

^{a} For comparison with $Mo_4Cl_{12}^{4-}$, a calculation was done with the experimental geometry of $Mo_2Cl_8^{4-}$, but with a Mo–Mo distance of 2.21 Å and 2 added electrons to give $\sigma^2\pi^4\delta^2\delta^{*2}$.

evident here recur in more complex form for the Tc clusters. Figure 1 shows the construction of Mo_4Cl_8 (see Appendix for geometry), an unbridged, more symmetrical analogue of $Mo_4Cl_8(PEt_3)_4$. In Figure 1, two $Cl_2Mo\equiv MoCl_2$ units interact to form Mo_4Cl_8. The orbitals of two isolated Mo_2Cl_4 units, drawn on the left of this figure, show the expected d orbital splitting pattern for a metal–metal bonded dimer: σ falls below two π orbitals, followed in order by $\delta(x^2-y^2)$, $\delta^*(x^2-y^2)$, $\delta(xy)$, and $\delta^*(xy)$. The two π^* orbitals, as well as σ^*, are too high in energy to appear in the figure. The π orbitals are slightly split because their π^* overlap with Cl p orbitals is different for the two different d orbital orientations. Likewise, $\delta(x^2-y^2)$ and $\delta(xy)$ are nondegenerate because of the crystal field of the chlorides—$\delta(xy)$ is strongly destabilized through σ antibonding interactions. The orbitals are filled through the δ levels, corresponding to Mo–Mo quadruple bonds.

Bringing the two fragments together gives the level ordering shown on the right of Figure 1. The extent of orbital splitting in each case can be understood from the topologies of orbital interaction. σ orbitals split very little; they interact primarily via the small torus of the z^2 orbital. $\pi(xz)$ splits more because of its π type interaction with the neighboring Mo_2Cl_4 fragment. $\pi(yz)$ interacts least (by δ overlap between dimers), while the δ type orbitals split the most, through σ overlap with the adjacent dimer. The lowest δ^* orbital is stabilized enough to become occupied in Mo_4Cl_8. The unbridged dimer of Mo_2Cl_8 can therefore be formulated as containing two triply bonded Mo_2 units held together by σ overlap of their individual δ and δ^* orbitals. Figure 2 demonstrates that adding the 4 bridging Cl^- ligands to Mo_4Cl_8
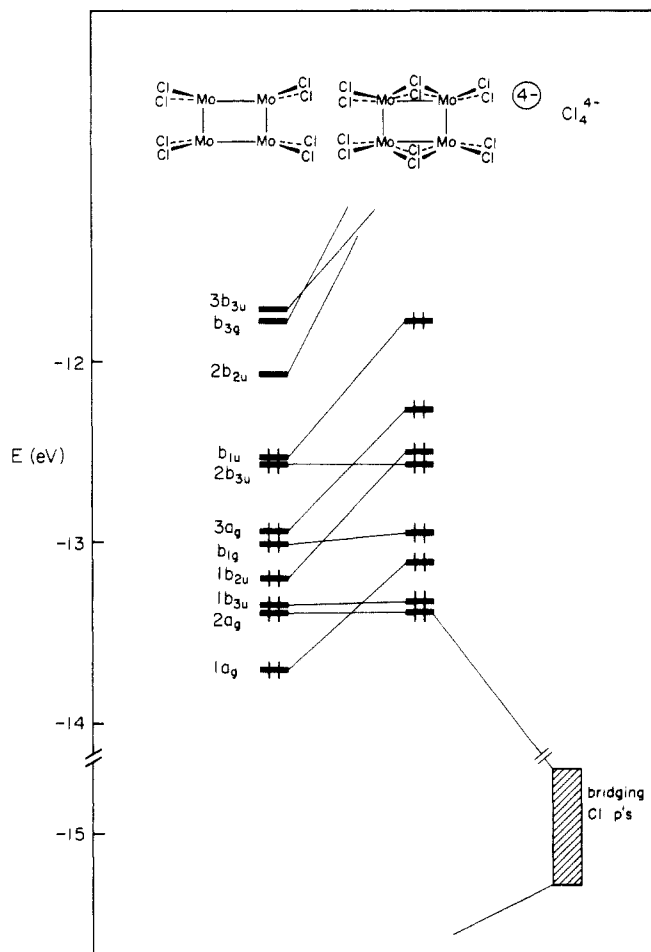
Figure 2. Adding four Cl^- bridges to Mo_4Cl_8 forms the $Mo_4Cl_{12}^{4-}$ analogue of McCarley's $Mo_4Cl_8(PEt_3)_4$[4] and leaves the description of metal–metal bonding the same as for Figure 1.

changes the level ordering but maintains the qualitative bonding description.

There is another way to make the picture of the bonding in the various molecules more precise. Each contains an Mo_2 entity, which has nicely defined σ, π, δ, δ^*, π^*, σ^* orbitals (and further s and p based σ and π combinations). For any molecule which contains an Mo_2 unit we can do a fragment molecular orbital (FMO) decomposition of the MOs of the molecule in terms of the Mo_2 orbitals. This is accomplished in Table II. σ and π orbitals are completely filled for each entry in the table. For Mo_2Cl_4, population of the δ orbital is larger than the δ^* occupation by 1.9 electrons. δ and δ^* occupations are more nearly equal in Mo_4Cl_8 and differ by only 0.16 for $Mo_4Cl_{12}^{4-}$. This implies that the δ bond in Mo_2Cl_4 is substantially weakened by dimerizing to form Mo_4Cl_8 and essentially nonexistent in $Mo_4Cl_{12}^{4-}$. $Mo_4Cl_{12}^{4-}$ is left with Mo≡Mo triple bonds along the rectangle's short sides with single bonds spanning the longer Mo–Mo distances. We should mention here that this picture of metal–metal bonding in $Mo_4Cl_8(PEt_3)_4$ was inferred already from spectroscopic data.[18]

Trimers of Dimers: $Tc_6Cl_{12}^{2-}$

One way to build the electronic structure of $Tc_6Cl_{12}^{2-}$ is to consider bringing together three Tc_2Cl_2 units and then adding the six bridging Cl^- ligands. Figure 3 shows the first step of the process, the interaction of three Tc_2Cl_2 fragments to form $Tc_6Cl_6^{4+}$.

The orbitals of Tc_2Cl_2, shown on the left of the figure, have an energy ordering similar to that of the Mo_2Cl_4 fragment just described. σ is the lowest energy orbital with two π's immediately above. The levels differ from the usual metal–metal bonded dimer

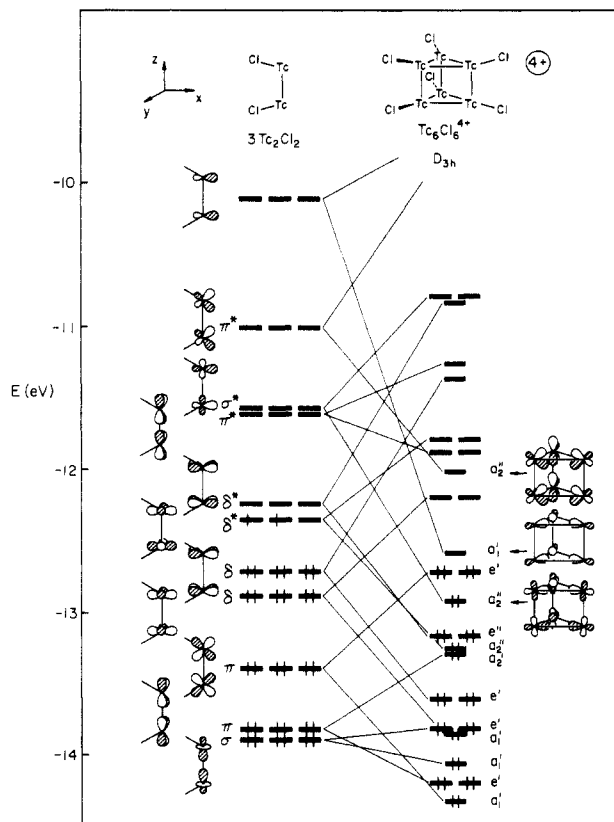(18) Ryan, T. R.; McCarley, R. E. *Inorg. Chem.* **1982**, *21*, 2072.

Figure 3. Interacting three Tc_2Cl_2 fragments to form trigonal prismatic $Tc_6Cl_6^{4+}$ results in three triply bonded dimers held together by overlap of their δ and δ^* orbitals.

orbitals by having *two* low-lying δ and δ^* orbitals instead of only one. This is because one member each of the δ and δ^* sets is usually pushed to high energy by a σ^* interaction with several ligands instead of just one. Interactions with ligand orbitals also explain the splitting within the π and δ sets. Tc xz is pushed above yz because of π^* interactions with the ligands. yz has δ symmetry with respect to the chlorine ligands and remains at low energy. Likewise, xy is driven to higher energy than x^2-y^2 because its antibonding π overlap with Cl p's is larger than the σ overlap between Cl orbitals and Tc x^2-y^2. π overlap is larger than σ in this case because bending the Cl up by 15° substantially reduces the σ overlap but leaves the π overlap almost unchanged. Similar reasoning applies to the π^* and δ^* orbitals, although mixing between σ^* and π^* complicates the picture. Also shown in Figure 3 is a high-energy orbital, mainly Tc s, hybridized away from the chlorine ligand by some admixture of p_x.

The level ordering shown on the right of Figure 3 results from interacting the three Tc_2Cl_2 fragments to form $Tc_6Cl_6^{4+}$. We do not draw out all the orbitals but simply note that each set of dimer levels splits into an a and an e set to give three levels resembling the Walsh orbitals of cyclopropane.[19] For the $\sigma(z^2)$ and radial $\pi(xz)$ and $\delta(x^2-y^2)$ orbitals, the splitting puts the totally bonding a combination below e. The completely antibonding a level is above the e set for yz and xy. We refer the reader to any of several sources for a more detailed description of the e orbitals.[19,20] The s orbital is pushed to still higher energy by mixing with lower lying orbitals of the same symmetry.

The bonding between dimeric fragments can be qualitatively understood from the magnitudes of the various level splittings in Figure 3. Dimer σ orbitals interact the least, whereas orbitals of δ symmetry are split the most because their lobes point toward neighboring dimeric units. For the electron filling appropriate

(19) Walsh, A. D. *J. Chem. Soc.* **1953**, 2266.
(20) (a) Albright, T. A.; Burdett, J. K.; Whangbo, M.-H. *Orbital Interactions in Chemistry*; Wiley-Interscience: New York, 1985. (b) Gimarc, B. M. *Molecular Structure and Bonding*; Academic: New York, 1979.
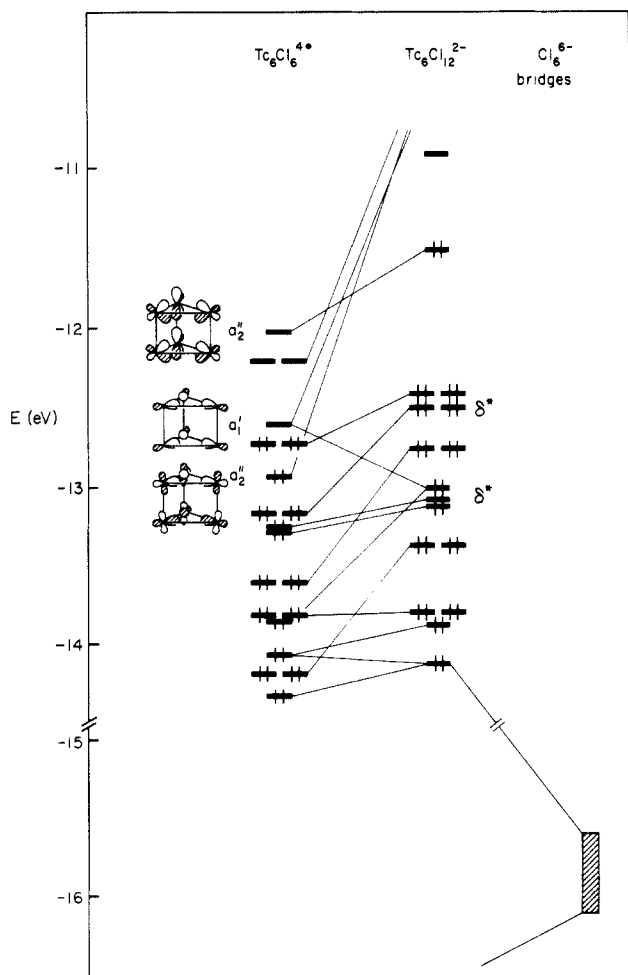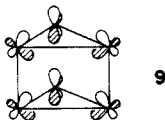
Figure 4. Adding bridging Cl⁻ ligands to $Tc_6Cl_6^{4+}$ gives a HOMO that is π antibonding within dimers and π bonding between them.

Figure 5. Energy levels of $Tc_6Cl_{12}^{2-}$ (a) and orbital contributions to Tc–Tc overlap population within Tc–Tc dimers (b) and between dimers (c).

Table III. Orbital Occupations for Tc_2 Fragment Orbitals

molecule	orbital occupations					
(fragment)	σ	π	δ	δ^*	π^*	σ^*
$Tc_6Cl_6^{4+}$	1.99	3.94	2.00	1.82	0.53	0.67
$Tc_6Cl_{12}^{2-}$	1.99	3.92	2.36	2.13	1.02	0.64
Tc_6Cl_{12}	1.99	3.92	2.36	2.13	0.74	0.45
$(Tc_2Cl_8^{4-})^a$	1.99	4.00	2.60	2.59	0.52	0.30

[a] Orbital occupations for the $Tc_2Cl_8^{2-}$ experimental geometry,[25] but with the Tc–Tc distance 2.21 Å and 2 electrons added to give an electron-rich triple bond.

for $Tc_6Cl_{12}^{2-}$, 32 d electrons, dimer σ and π orbitals that are bonding *and* antibonding between Tc_2Cl_2 fragments are filled. The dimers in $Tc_6Cl_6^{4+}$ are held together by σ bonds formed from local dimer δ and δ^* orbitals (the double prime labels an orbital as antisymmetric to σ_h and therefore antibonding within Tc–Tc dimers). In addition, an orbital with σ^* character within the Tc_2Cl_2 dimers is filled.

Adding the bridging chloride ligands perturbs this bonding description very little (see Figure 4). The most significant changes occur among levels near the HOMO–LUMO gap, resulting in depopulation of the σ^* level, a_2''. The HOMO becomes a level of π^* character within the dimers and bonding between them. This orbital is important, for it is partially depopulated on going from $Tc_6Cl_{12}^{2-}$ to $Tc_6Cl_{14}^{3-}$. The a_2'' MO is shown in **9**. Removing

electrons from this orbital should contract the short Tc–Tc bonds and lengthen bonds bordering the triangular faces. This is consistent with observed structural differences between $Tc_6Cl_{12}^{2-}$ (Tc≡Tc = 2.21 Å, Tc–Tc = 2.57 Å; 32e⁻) and $Tc_6Cl_{14}^{3-}$ (Tc≡Tc = 2.16 Å, Tc–Tc = 2.70 Å; 31e⁻).

We find a significant (0.7 eV) gap between the HOMO and the LUMO for the 32e⁻ system. This is probably large enough to assure a singlet ground state for the cluster. Experimentally weak paramagnetism has been reported.[1b,c]

Figure 5 clarifies the bonding, nonbonding, or antibonding nature of the d block levels of $Tc_6Cl_{12}^{2-}$. The figure shows the cluster analogue of the COOP curve, a tool developed to describe the levels of an extended three-dimensional solid.[21] The horizontal
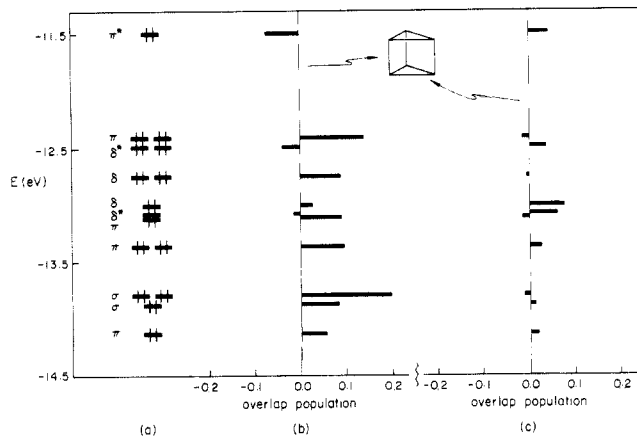
lines in parts b and c of Figure 5 represent contributions to Tc–Tc overlap populations from the levels marked in Figure 5a. Figure 5b is the overlap population within Tc–Tc dimers and Figure 5c that between dimers. Bonding within dimers, as measured by overlap populations, is much stronger than bonding between dimers: more levels are bonding in Figure 5b than in Figure 5c, and their contributions to the overlap population are larger. The levels largely reponsible for bonding between dimers are the upper seven levels with positive Tc–Tc overlap population in Figure 5c. These include the HOMO (π^*), 3δ^*, one δ, and 2 orbitals labeled as π. The π orbitals have mixed strongly with a δ set of the same symmetry, but Figure 5 shows that the earlier picture of dimer aggregation by overlap of purely δ and δ^* orbitals is oversimplified.

The occupations of bare Tc_2 fragment orbitals displayed in Table III emphasize that the description of $Tc_6Cl_{12}^{2-}$ in terms of Tc≡Tc units is a good one. σ and π are always filled, and occupations of δ and δ^* are nearly equal for $Tc_6Cl_{12}^{2-}$ and Tc_6Cl_{12}.

The drop in π^* and σ^* occupations upon oxidizing $Tc_6Cl_{12}^{2-}$ to Tc_6Cl_{12} highlights the π^* and σ^* character (mainly π^*) of the HOMO for $Tc_6Cl_{12}^{2-}$. The 0.9-eV gap just below the HOMO, as well as its antibonding character within Tc_2 dimers, suggests that a 2-electron oxidation to reach an equally good electron count of 66 (30 metal d electrons) should be possible.

To put it another way, the HOMO of $Tc_6Cl_{12}^{2-}$ is net Tc–Tc antibonding—its π^* nature within a dimer wins out over its bonding within a triangle. If we had to give an answer to how many framework bonding orbitals there are in these trigonal prismatic M_6Cl_{12} structures, we would say 30, 15 pairs. This is what we entered in Table I.

Note that this magic number is exactly what one would get from a localized valence bond structure count for **10**. The equivalent orbital symmetries match MO symmetries, too.

There is a further isomeric possibility that springs to mind, once one recalls the common $Re_3Cl_{12}^{3-}$ structural type.[3] This is an alternative trigonal prismatic structure, **11**, realizable perhaps as $Tc_6Cl_{18}^{6-}$, **12**. The interconversion of **10** and **11** is strongly for-

(21) For some earlier uses of the COOP curve, see: (a) Wijeyesekera, S. D.; Hoffmann, R. *Organometallics* **1984**, *3*, 949. (b) Saillard, J.-Y.; Hoffmann, R. *J. Am. Chem. Soc.* **1983**, *105*, 2006.
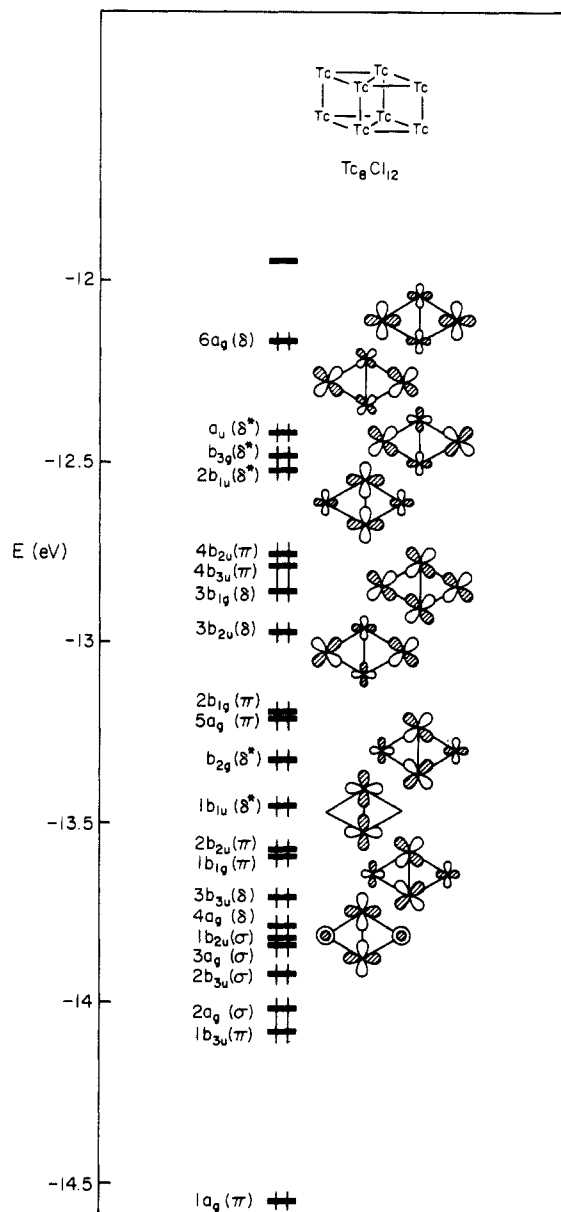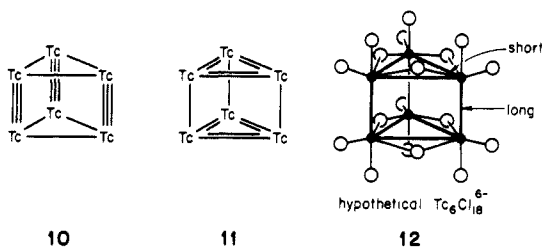
Figure 6. Energy levels of a Tc_8Cl_{12} model for Tc_8Br_{12}, **3**.

bidden, involving several level crossings. This opens up the possibility of isolable isomeric molecules.

10 **11** **12**

Finally, we note that $Tc_6Cl_{12}{}^{2-}$ also shows a 0.6-eV HOMO–LUMO gap if electrons were added to it so as to reach a total of 88 electrons, close to the usual electron count of 90 (cf. $Rh_6C(CO)_{15}{}^{2-}$, Table I). For Tc–Tc single bond distances of 3.0 Å, this gap widens to 1.6 eV, while the gap for 68 electrons disappears. Strong metal–metal bonding simply opens a second gap dividing Tc≡Tc bonding and antibonding levels in $Tc_6Cl_{12}{}^{2-}$.

Table IV. Orbital Occupations for Tc_2 Fragment Orbitals

molecule	Tc type	orbital occupations					
		σ	π	δ	δ^*	π^*	σ^*
$Tc_8Cl_{12}{}^a$	interior	1.99	3.92	2.47	2.25	0.83	0.46
	exterior	1.99	3.95	2.48	2.13	0.67	0.38
$Tc_2Cl_8{}^{4-\ b}$		1.99	4.00	2.60	2.59	0.52	0.30

^{a} Tc_8Cl_{12}, **3**, contains 2 different types of Tc atoms. "Interior" refers to atoms in the shared prism face, without terminal ligands. "Exterior" refers to atoms with terminal ligands. ^{b} See Table III, footnote *a*.

Table V. Parameters for the Extended Hückel Calculations

	orbital	H_{ii} (eV)	$\zeta_1(C_1{}^a)$	$\zeta_2(C_2{}^a)$
Mo	4d	−12.30	4.54 (0.5899)	1.90 (0.5899)
	5s	−9.66	1.956	
	5p	−6.36	1.90	
Tc	4d	−12.82	4.90 (0.5715)	2.094 (0.6012)
	5s	−10.07	2.018	
	5p	−5.40	1.984	
Cl	3s	−30.0	2.033	
	3p	−15.0	2.033	

^{a} Coefficients in the double-ζ orbital expansion.

Face-Sharing Trigonal Prisms: Tc_8Br_{12}

We do not discuss the orbitals of Tc_8Br_{12} in great detail because the Tc–Tc bonding is similar to that in $Tc_6Cl_{12}{}^{2-}$. We can briefly point out the differences with the help of Figure 6, the energy levels of a Tc_8Cl_{12} model for Tc_8Br_{12}.

The short Tc–Tc bonds are electron-rich triple bonds similar to the triple bonds within "dimers" in $Tc_6Cl_{12}{}^{2-}$ (see Table IV). Tc_2 units in the Tc_8Cl_{12} model are bound together by overlap of *five* δ and δ^* orbitals. Four δ and four δ^* orbitals can be associated mainly with bonds around the rhomboidal top and bottom faces of the cluster. The remaining δ and δ^* orbitals ($4a_g$ and $1b_{1u}$) are concentrated on atoms located in the prisms' shared face and can be identified with the bonds bisecting rhomboidal faces. The absence of terminal Br ligands on these technetiums is what distinguishes them from the others and keeps $4a_g$ and $1b_{1u}$ at low energy.[22]

Appendix

All calculations were performed with the extended Hückel method[23] with the parameters listed in Table V. Mo parameters were taken from previous calculations.[24] Technetium exponents and expansion coefficients are from Basch and Gray,[25] appropriately normalized. Technetium H_{ii}'s were determined by charge iteration on $Tc_2Cl_8{}^{2-}$ in the experimental geometry,[26] using *A*, *B*, and *C* values from Baranovskii and Nikol'skii.[27] Experimental geometries were used for all calculations, except that Cl's were bent away from the Mo≡Mo bond by 15° for $Mo_4Cl_{12}{}^{4-}$.

Registry No. 1, 101178-51-2; **2**, 103752-27-8; [$TcBr_{12}$]Br[($H_2O)_2H$], 84558-05-4; Tc, 7440-26-8.

(22) For a preliminary account of our work see: Wheeler, R. A.; Hoffmann, R. *Angew. Chem.*, in press.

(23) (a) Hoffmann, R.; Lipscomb, W. N. *J. Chem. Phys.* **1962**, *36*, 2179, 3489; **1962**, *37*, 2872. (b) Hoffmann, R. *Ibid.* **1963**, *39*, 1397. (c) Ammeter, J. H.; Bürgi, H.-B.; Thibeault, J. C.; Hoffmann, R. *J. Am. Chem. Soc.* **1978**, *100*, 3686.

(24) Tatsumi, K.; Hoffmann, R. *Inorg. Chem.* **1980**, *19*, 2656.

(25) Basch, H.; Gray, H. B. *Theor. Chim. Acta* **1966**, *4*, 367.

(26) Cotton, F. A.; Daniels, L.; Davison, A.; Orvig, C. *Inorg. Chem.* **1981**, *20*, 3051.

(27) Baranovskii, V. I.; Nikol'skii, A. B. *Teor. Eksper. Khim.* **1967**, *3*, 527; *Theor. Exper. Chem.* **1967**, *3*, 309.